Int. J. Electrochem. Sci., 13 **(2018)** 10635 – 10641, doi: 10.20964/2018.11.23

International Journal of
ELECTROCHEMICAL
SCIENCE
www.electrochemsci.org

Short Communication

A Study of Superior Photocatalytic Properties of Synthesized TiN through a Facile Approach

Huancong Shi[1*], *Yujie Ma*[1], *Min Huang*[1], *Mingqi Cui*[1], *Shuxian Wei*[1], *linhua Jiang*[1*] *Yuanhui Zuo*[1, 2*]

[1] Department of Environment Science and Engineering, Shanghai Key lab of Modern Optical Systems, University of Shanghai for Science and Technology, Shanghai 200093, China
[2] College of Environmental Science and Engineering, Tongji University, Shanghai 200092, China
[*]E-mail: hcshi@usst.edu.cn lhjiang@usst.edu.cn zyh06101@163.com

Received: 25 June 2018 / *Accepted:* 24 august 2018 / *Published:* 1 October 2018

The synthesized TiN (s-TiN) with superior catalytic activity was fabricated through a simple, low-cost, and non-toxic process as a potential material of waste water treatment. The photocatalytic performance of s-TiN was estimated by chemical reduction of Cr(VI) and photo degradation of RhB with existence of visible light. For s-TiN, the removal rate of Cr(VI) was 98% within 1 minute and the photo degradation of RhB reached to 99.7% within 4 minutes. However, for the purchased TiN (p-TiN), the removal rate of Cr(VI) was 17% and the degradation rate of RhB was only 1%. The excellent photocatalytic activity is owing to the increased molecular adsorption, visible light absorption and effective charge separation. Furthermore, another interesting discovery is that the metal Zinc was produced along with TiN synthesis on the inside crucible cover simultaneously.

Keywords: TiN, Sol-gel synthesis, photocatalytic activity

1. INTRODUCTION

TiN has received intensive attention due to its excellent physical and chemical properties, such as high hardness, wear, and density, but low electrical resistivity and corrosion resistivity [1-4]. TiN has been widely used in the field of protective coatings for cutting and forming tools. Several methods utilized the deposition of TiN thin films with desirable properties, such as physical vapor deposition (PVD) [5-7], chemical vapor deposition (CVD)[6], and atomic layer deposition method [8,9]. There has been few reports of TiN used as highly active photocatalysts in field of wastewater treatment.

In this study, we successfully extended the facile and prolific strategy (Sol-gel synthesis) into a single-crystal TiN with floc surface, and it exhibited excellent photocatalytic activity in Cr(VI) reduction and RhB degradation comparing with p-TiN under UV-visible light irradiation. As a result,

the remarkable photocatalytic activity are caused by the enlarged specific surface area (SSA) and efficient charge separation and transport. With these merits, s-TiN exhibits great potentials in various fields of solar cells, lithium batteries, sensors and photocatalysts. In addition, pure Zinc metal was produced on the inside cover of crucible during the synthesis process of TiN. We developed a material synthesis process in which TiN and pure Zn were generated simultaneously.

2. EXPERIMENTAL METHODS

2.1 Preparation of TiN

The g-C_3N_4 was synthesized by simple calcination of carbamide at 550 °C for 4 hours in a covered alumina crucible. A soft template of ionic surfactants adopted cetyltrimethyl ammonium bromide (CTAB). All the chemicals are analytical grade (99%), including deionized water.

The s-TiN was prepared as follows: firstly, 1.2 g of g-C_3N_4 with 0.2 g of surfactant (CTAB) were dissolved in 10 mL deionized water with sonication for 30 min at 50 °C. Secondly, Zinc acetate dihydrate (2.25 g) and titanium iso-propoxide (3.14 mL) were mixed and dissolved in 3.33 mL acetic acid (CH_3COOH) and blended at mole ratio of Zn : Ti (1 : 0.9).[10] Then, both solutions were mixed under sonication for 10 mins and heated around 50 °C, and blended the surfactant (CTAB) under sonication for another 10 mins. Thirdly, a transparent sol was produced in an air flow oven at 50 °C after heating several hours. The product gel was heated at 120 °C for 10 hours in order to remove the acetic acid thoroughly. Finally, s-TiN powders was obtained after the gel was calcined at 900 °C and equilibrated for 2 hours with a heating rate of 10 °C/min.

2.2 Materials Characterization

XRD patterns were recorded on a Rigaku D/MAX-2495VB/PC diffractometer under the following conditions: θ–2θ mode, Cu Kα1 radiation (λ = 1.5406 Å). The SEM images were recorded using an FEI XL-30 scanning electron microscope, 25 kV. The Brumauer–Emmett–Teller (BET) surface areas were recorded on a BeiShiDe 3H-2000PS4 device at -196 °C. Total pore volume (Vt) was determined at relative pressure of 0.98. Last but not least, Electro-chemical impedance spectroscopy (EIS) tests were performed at open circuit potential over the frequency range between 100 kHz and 0.1 Hz. The detailed parameters were: initial E = 2.72 V (C_3N_4); 2.94 V (p-TiN); 3.07 V (s-TiN); High Frequency = $1e^{+6}$ Hz, Low Frequency = 0.1 Hz; Imp SF; Amplitude = 0.005V; Quiet Time = 2 sec; Cycles (.1-1Hz) = 1 Hz.

2.3 Photocatalytic performance

Photocatalytic performance of s-TiN was tested by chemical reduction of Cr(VI) and catalytic degradation of RhB with existence of visible light. For the reduction of Cr(VI), 50 mg of s-TiN and p-TiN with 30 mL of Cr(VI) solution (40 ppm) were added into the reactor. The pH value was adjusted

to 2–3 with HNO_3. Then, the solution was irradiated by a 300W Xe lamp with a 420 nm cutoff filter. At scheduled time intervals, 1-2 ml solution was sampled and separated with centrifugation. The Cr(VI) concentrations were measured with UV–vis spectrophotometer at its optimized wavelength of 540 nm with the diphenylcarbazide method (DPC) [11]. Similarly, the photo degradation tests of RhB was performed with 50 mg of s-TiN immersed into 30 mL of RhB solution (50 ppm). The process and parameters were similar to those for the reduction of Cr(VI). During the photocatalytic degradation, 1 mL solution was collected at every minute (except 30 seconds for the first sample) and centrifuged to separate the photocatalysts. The time-resolved concentration of RhB was tested with record of the absorbance at 554 nm with an UV-vis spectrophotometer.

3. RESULTS AND DISCUSSION

The SEM and XRD patterns of the g-C_3N_4, s-TiN, p-TiN and Zn were shown in Fig. 1a-c. The surface was smooth of p-TiN without uniform size (Fig.1a), but the surface of the floc-like s-TiN (Fig.1b) was coarser than p-TiN. The XRD patterns of the prepared samples were shown in Fig. 1c. The diffraction pattern of s-TiN indicated that the peaks are indexed as the cubical TiN phase (JCPDS 38-1420). The XRD pattern of s-TiN contains sharper diffraction peaks than p-TiN, which conformed that s-TiN owns better crystallinity. Furthermore, XRD pattern of Zn demonstrated that as-prepared Zinc is mono-component. We synthesized pure single-crystal TiN and pure Zn simultaneously through a simple one-step process.

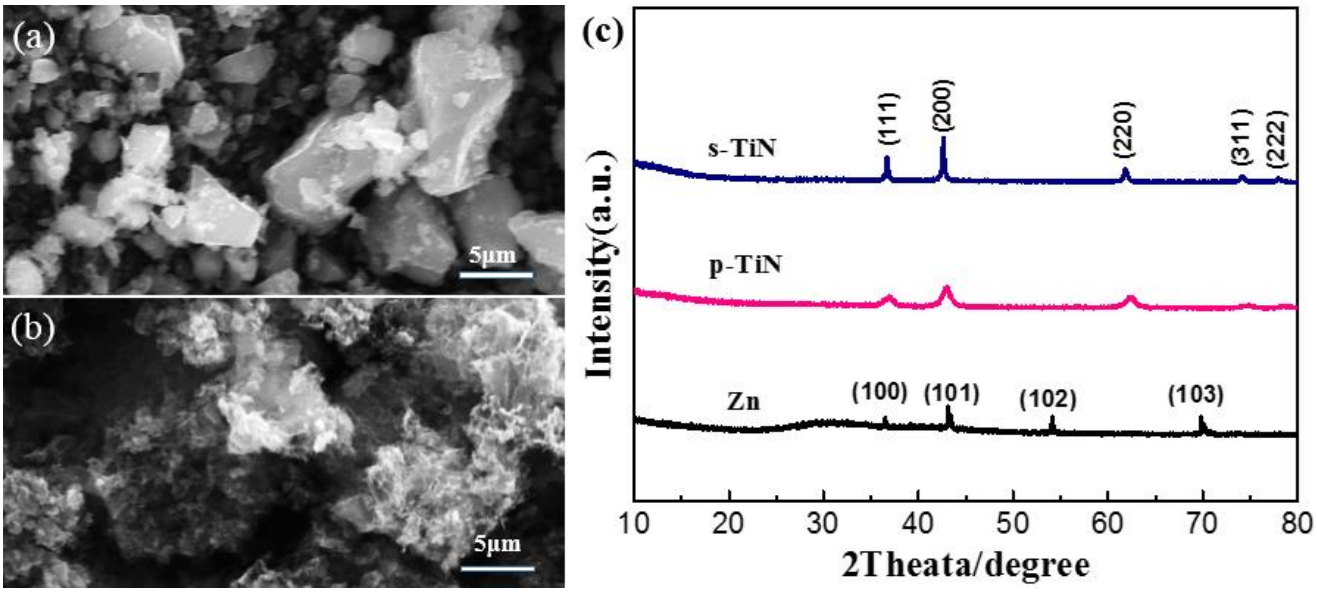

Figure 1. SEM images of (a) p-TiN and (b) s-TiN. XRD patterns (c) of s-TiN, p-TiN and Zn.

Fig. 2a displayed the N_2 adsorption desorption isotherms and pore size distribution curves (inset) of s-TiN, p-TiN and g-C_3N_4. The average pore diameters of all the samples are 7.54 nm, 13.45

nm and 38.25 nm. The s-TiN exhibited a typical IV isotherm with a H3-type hysteresis loop, representing the mesoporous structure from classification of IUPAC [12]. The BET surface area of p-TiN was only 1.22 m^2g^{-1}, which prove itself as a poor photocatalyst. On the contrary, the SSA of s-TiN was 129.95 m^2g^{-1}, which is about 100 times bigger than p-TiN, and higher than g-C_3N_4 (70.78 m^2g^{-1}). The total pore volume of the s-TiN was 0.2451 cm^3g^{-1}, much larger than that of p-TiN of 0.0041 cm^3g^{-1}, which indicated the fluffy state of s-TiN. It was reasonable that the s-TiN promotes the photo catalysis with much more active sites along with enhancement of the charge transfer.

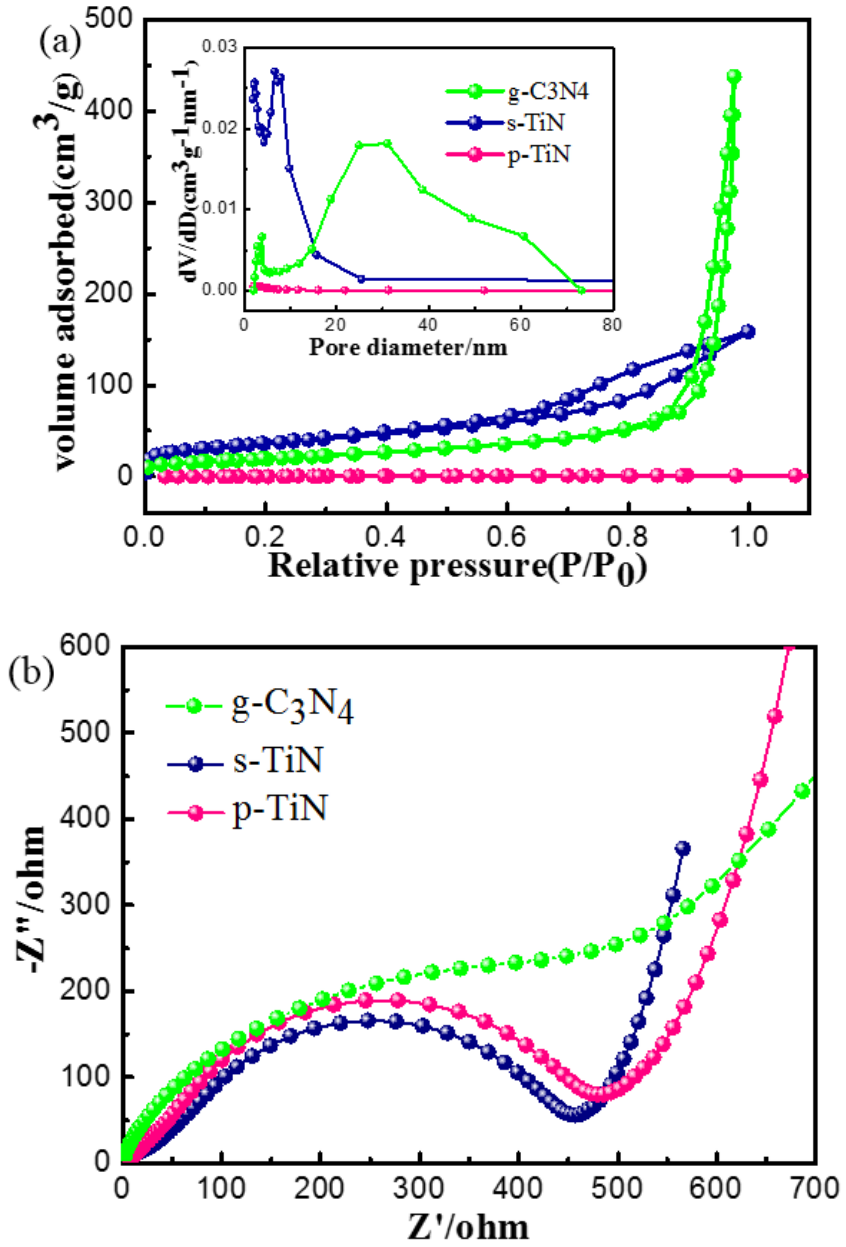

Figure 2. (a) The pore size distribution curves(inset) of g-C_3N_4, s-TiN and p-TiN from N_2 adsorption-desorption isotherms, (b) EIS spectra of photocatalysts of g-C_3N_4, s-TiN and p-TiN, the smaller radius the better.

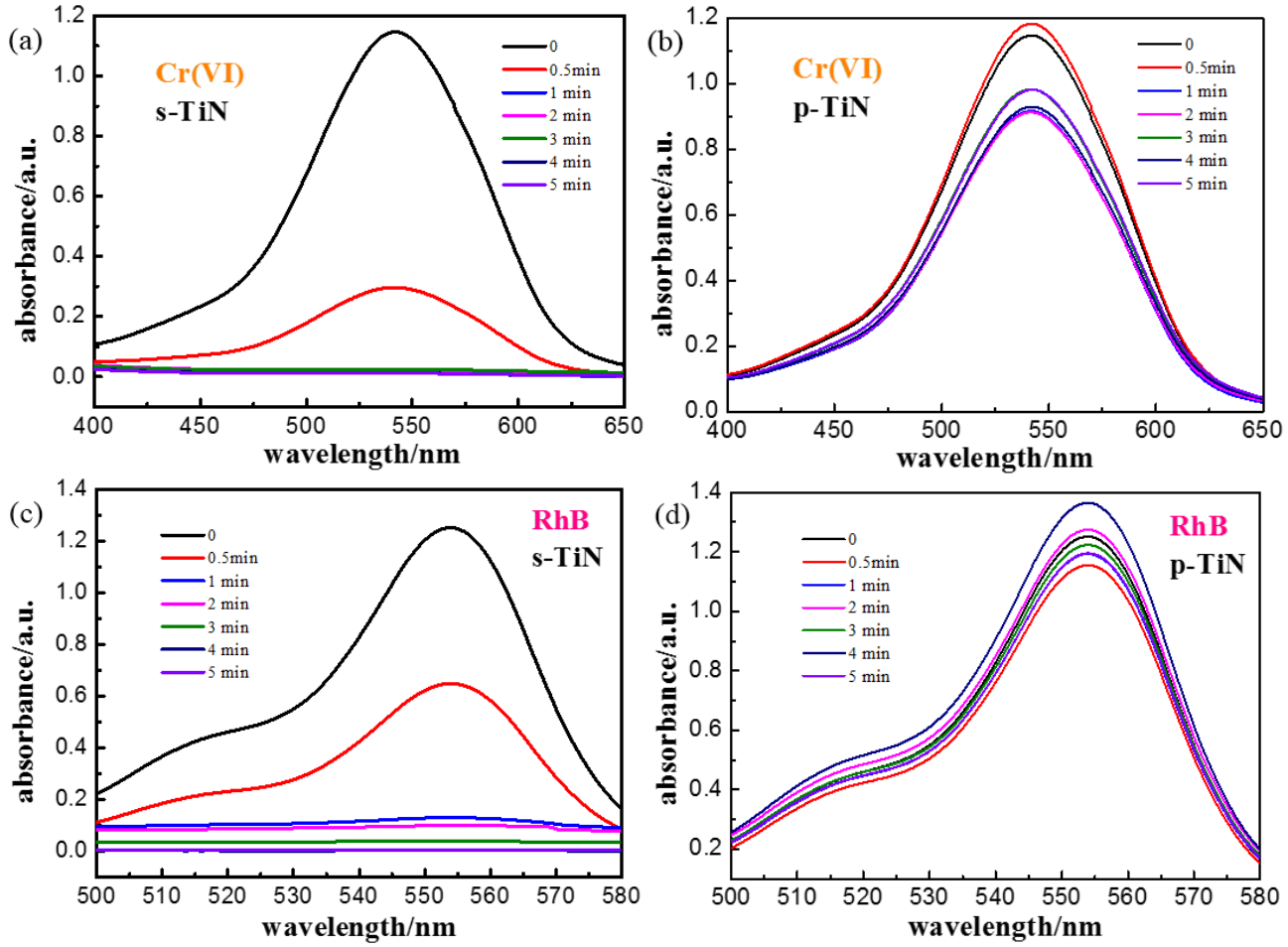

Figure 3. Evolution of the Cr(VI) UV-Vis spectra vs. time with s-TiN (a) and p-TiN (b), Evolution of the RHB UV-Vis spectra with time in presence of s-TiN (c) and p-TiN (d).

The arc radius of s-TiN on the EIS Nyquist plot was the smallest (Fig. 2b) among s-TiN, p-TiN and g-C_3N_4, demonstrating that s-TiN could greatly reduce interfacial charge transfer resistance, along with enhanced electron-hole interfacial separation / transfer efficiency [15].

Fig. 3 presented the temporal evolution of the UV Visible spectra of pollutants with existence of s-TiN and p-TiN. The photocatalytic activity of s-TiN was evaluated by removal of the $K_2Cr_2O_7$ and RhB solutions under visible light irradiation. There was no dark adsorption experiments for this study, since pollutant concentrations did not show significant decrease within 5 mins. In addition, our photocatalytic experiment only took 1-5 minutes, and it is insignificant to perform absorption experiments. Instead, there are a variety of nanostructures with different structures and ingredients for the reduction of Cr(VI) and photo-degradation of RhB such as C fibers@MoS_2 nanoplates core-shell composite [15], g-C_3N_4/MIL-53(Fe) [16], TiO_2/CdS films [17] and the anatase/rutile mixed-phase TiO_2 hollow spheres [18] have been reported. The C fibers@MoS_2 nanoplates core-shell composite [15] reached 50.83% Cr(VI) reduction within 160 minutes. On the other hand, the absorption in the dark on RhB over the C fibers@MoS_2 NPCSC was about 22.55%. After 70 min, the photocatalytically degraded RhB over the present composite catalyst reached 24.23% [15]. The g-C_3N_4/MIL-53(Fe)-(3% CN) [16] reduced Cr(VI) to 80% within 120 minutes. The photocatalytic performance of TiO_2/CdS

films [17] achieved a reduction rate of 60% for 50 min, 80% for 120min, and highest rate of 93% for 240 min. The anatase/rutile mixed-phase TiO_2 hollow spheres [18] degraded RhB at 80% for 60 mins and about 100% for 90 mins. In Summary, the photocatalytic efficiency of these heterostructures usually takes 1-2 hours to complete 80% of the reduction and photo-degradation. These works are inferior to our synthesized s-TiN, taking minutes. From Fig. 3(a, b), approximately 17% of Cr(VI) was reduced by the p-TiN and 98% by the s-TiN under visible light irradiation within 1 min. Fig. 4a showed the linear fitting of a pseudo-first-order kinetics based on the experimental data of s-TiN, p-TiN and g-C_3N_4. The rate constants *k* were generated directly from the slope of straight-line plots of $\ln(C/C_0)$ versus irradiation time (t). The *k* followed the order: s-TiN (4.0844 min^{-1}) > g-C_3N_4 (0.04331 min^{-1}) > p-TiN (0.0342 min^{-1}). The s-TiN exhibits the best photocatalytic activity among s-TiN, p-TiN and g-C_3N_4.

The p-TiN showed nearly zero photocatalytic activity for the RhB degradation. However, the s-TiN exhibited enhanced photocatalytic degradation efficiency (Fig. 3c, d). The degradation of RhB followed a pseudo-first order reaction: $\ln(C/C_0) = -kt$ (Fig. 4b). The rate constant k followed the order of: s-TiN (1.1566 min^{-1}) > g-C_3N_4 (0.10507 min^{-1}) > p-TiN (0.01805 min^{-1}). Consequently, the s-TiN exhibited the highest photocatalytic activity in RhB degradation process. The g-C_3N_4 has little effect comparable to p-TiN [13,14].

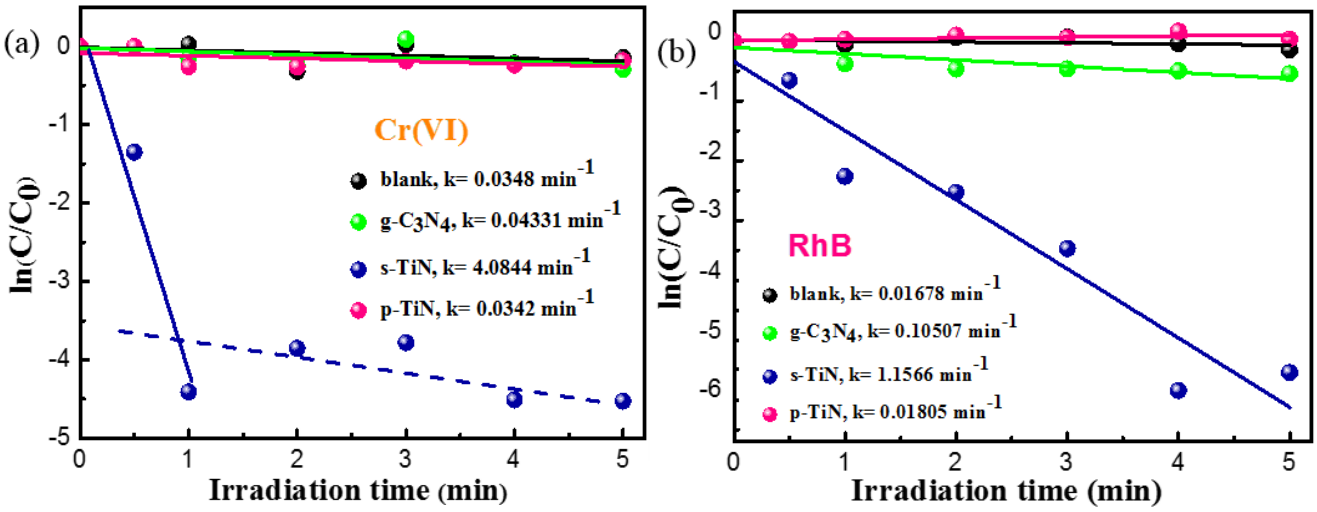

Figure 4. The photocatalytic reaction kinetics of Cr(VI) (a) and RhB (b) with pseudo-first order.

4. CONCLUSIONS

The synthesized-TiN (s-TiN) photocatalyst was successfully produced via a sol-gel synthesis method. It showed excellent photocatalytic activity for reduction rates of Cr(VI) and degradation rates of RhB in the presence of visible light irradiation. The material of s-TiN acted as an attractive potential photocatalysts in the field of waste water treatment.

ACKNOWLEDGEMENTS
This work was supported with National Natural Science Foundation of China (NSFC. 21606150, 61775139), and Young Eastern Scholar (QD2016011) and complement (QD2016011-005-11).

References

1. J. E. Sundgren, *Thin Solid Films.*, 128 (1985) 21.
2. N. Savvides, B. Window, *J. Appl. Phys., 64* (1988) 225.
3. L. Hultman, *Vacuum.*, 57 (2000) 1.
4. E. Kelesoglu, C. Mitterer, M. Urgen, *Surf. Coating, Technol.,* 160 (2002) 82.
5. J. Narayan, P. Tiwari, X. Chen. *Appl. Phys. Lett.*, 61 (1992) 1290.
6. S. R. Kurtz, R. G. Gordon, *Thin Solid Films,* 140 (1986) 277.
7. S. Fortuna, *Thin Solid Films.,* 377 (2000) 512.
8. X. M. Ma, D. H. Zhu, D. Z. Mo, *Int. J. Electrochem. Sci.,* 10 (2015) 7941.
9. L. F. Cui,T. T. Pu, X. Y. Fang, *Int. J. Electrochem. Sci.,* 13 (2018) 4981.
10. S. Perween, A. Ranjan, *Sol. Energ. Mat. Sol. C.,* 168 (2017) 148.
11. X. Liu, J. Liu, H. Chu, *Applied Surface Science.,* 347 (2015) 269.
12. J. Liu, X. Liu, J. Li, *Rsc. Advances.*, 4 (2014) 38594.
13. L. Cao, R. Wang, D. Wang, *Mater. Lett.,* 149 (2015) 50.
14. Y. Jing, X. M. Hu, C. Y. Shao, *Int. J. Electrochem. Sci.,* 12 (2017) 9311.
15. H. Li, Z. J. Peng, M. Wang, Z. Y. Zhao, C. B. Wang and X. L. Fu, *J. Alloys Compd.,* 753 (2018) 378.
16. Y. Huang, N. Ling, X. D. Zhang, M. H. Wu and L. Tang, *Appl. Surf. Sci.*, 425 (2017) 107.
17. L. Shi, T. Wang, H. B. Zhang, K. Chang, X. G. Meng, H. M. Liu and J. H. Ye, *Adv.Sci.*,2 (2015) 1.
18. W. Bao, Q. L. Kang, C. Liu, J. Z. Ma, *Mater. Lett.*,214 (2018) 272.

© 2018 The Authors. Published by ESG (www.electrochemsci.org). This article is an open access article distributed under the terms and conditions of the Creative Commons Attribution license (http://creativecommons.org/licenses/by/4.0/).